A 1.0 μm Cylindrical Vector Beam Fiber Ring Laser Based on A Mode Selective Coupler

Jie Wang, Hongdan Wan, Han Cao, Yu Cai, Bing Sun, Zuxing Zhang, Lin Zhang

***Abstract*—We propose and demonstrate a continuous-wave all-fiber ring laser generating cylindrical vector beams (CVBs) using a MSC as transverse mode converter and mode splitter. The MSC is fabricated by a novel method free of pre-tapering, achieving LP_{11} mode with a high purity of > 96% near the wavelength of 1064 nm. The CVB fiber laser operates at a center wavelength of 1053.9 nm, with a 3 dB linewidth of less than 0.04 nm and a signal-to-background ratio of > 60 dB. The laser slope efficiency is > 9%. The radially and azimuthally polarized beams can be switched by adjusting the polarization controllers in the fiber ring cavity, with a high mode purity measured to be > 96%.**

***Index Terms*—Cylindrical vector beams, optical fiber lasers, mode converter.**

I. Introduction

The cylindrical vector beams (CVBs) includes radially and azimuthally polarized beams [1]. Due to their characteristic of unique axial symmetry in both amplitude field and polarization, CVBs have been widely used in particle physics [2], optical tweezers [3], material processing [4] high-resolution metrology [5], and surface plasmon excitation [6]. Especially the radially polarized beam, which is attracting more and more attention.

Various kinds of continuous-wave (CW) CVB generation techniques have been demonstrated with the use of certain spatial polarization selective elements introduced into the laser cavity, such as dual conical prism [7], birefringent components, [8], spatial-light modulator (SLM) [9], and sub-wavelength gratings [10]. As compared with using certain spatial polarization selective elements, all-fiber CVB generation method has the advantages of low cost, high compactness and efficiency [11], [12]. At present, two all-fiber methods are used. The first one is using offset splicing spot (OSS) method to generate high-order mode and few-mode fiber Bragg grating (FM-FBG) as the transverse-mode selector. Using this method, CW CVBs and pulsed CVBs based on mode-locking and Q-switched techniques are achieved [13]-[16]. However, high-order modes are excited by lateral misalignment between single mode fiber (SMF) and few mode fiber (FMF) which introduces insertion loss into fiber cavity and deteriorates slope efficiency of the CVB lasers [17]. The second method is using the mode selective coupler (MSC) as the transverse mode converter and splitter inside the laser cavity, as compared with the OSS, the fiber laser slope efficiency can be effectively improved [17], [18]. In Reference [18] we demonstrated a passively mode-locked fiber laser generating pulsed CVB based on an all-fiber MSC fabricated by pre-tapered technique, operating near a wavelength of 1550 nm. However, the laser slope efficiency is still limited to about 3.1%. Efforts are still needed to improve the laser slope efficiency as well as to extend the laser operating wavelength with a high CVB purity. Furthermore, the MSC's fabrication technology is relatively complex due to the pre-tapered process [19]-[21].

In this paper, firstly, we theoretically and experimentally present a novel all-fiber MSC capable of exciting LP_{11} mode in TMF with high mode purity and low loss. Then, we demonstrate a high slope efficiency CW CVB fiber laser based on the MSC near a wavelength of 1.0 μm with an ultra-high mode purity. To the best of our knowledge, this is the first report on CW CVB fiber laser with high efficiency and mode purity near a wavelength of 1.0 μm, using an all-fiber MSC fabricated free of pre-tapering. All these results are attractive for developing CVB lasers with high power for further potentially applications many applications in material processing and micro-machining [22], [23].

II. MSC Working Principle and Fabrication

The basic structure of the MSC is depicted in Fig. 1. It consists of a two mode fiber (TMF) and a SMF (core/cladding diameter = 6.2/125 μm, NA = 0.14). The conventional single mode telecom fiber (SMF-28, core/cladding diameter = 8.2/125 μm, NA = 0.14) is used as the TMF at wavelength of 1064 nm.

Manuscript received. This work was supported by National Natural Science Foundation of China (11704199), National Science Foundation of Jiangsu Province (BK20150858, BK20161521), the Postgraduate Research & Practice Innovation Program of Jiangsu Province (KYCX17_0746), the Distinguished Professor Project of Jiangsu (RK002STP14001), the Talents Projects in Nanjing University of Posts and Telecommunications (NY214002, NY215002) and the STITP of NUPT (XZD2017040). (Corresponding authors: Hongdan Wan and Zuxing Zhang).

Hongdan Wan is with the Advanced Photonic Technology Lab, Nanjing University of Posts and Telecommunications, Nanjing 210023, China (e-mail: hdwan@njupt.edu.cn).

Zuxing Zhang is with the Advanced Photonic Technology Lab, Nanjing University of Posts and Telecommunications, Nanjing 210023, China and also with Aston Institute of Photonic Technologies, Aston University, Birmingham B4 7ET, UK (e-mail: zxzhang@njupt.edu.cn).

Jie Wang is with the Advanced Photonic Technology Lab, Nanjing University of Posts and Telecommunications, Nanjing 210023, China.

Han Cao and Bing Sun are with the Advanced Photonic Technology Lab, Nanjing University of Posts and Telecommunications, Nanjing 210023,China.

Lin Zhang is with the Advanced Photonic Technology Lab, Nanjing University of Posts and Telecommunications, Nanjing 210023, China and also with Aston Institute of Photonic Technologies, Aston University, Birmingham B4 7ET, UK (e-mail: l.zhang@aston.ac.uk).

This article has been accepted for publication in a future issue of this journal, but has not been fully edited. Content may change prior to final publication. Citation information: DOI 10.1109/LPT.2018.2797990, IEEE Photonics Technology Letters

The principle of the coupler is to phase match the fundamental mode in the SMF with a high-order mode in the TMF, and achieve fundamental mode conversion to high-order modes [21].

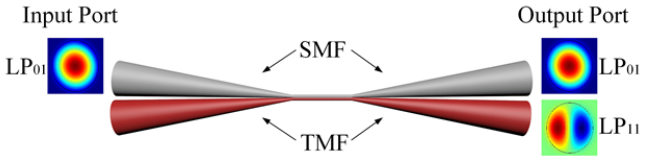

Fig. 1. Schematic of the MSC. The LP_{01} mode is launched into the SMF input port, the LP_{11} mode is expected to be excited at the TMF output port, while the uncoupled LP_{01} mode will propagate along the SMF.

According to the coupling mode equation [24]:

$$\frac{dA_1(z)}{dz} = i(\beta_1 + C_{11})A_1 + iC_{12}A_2 \quad (1)$$

$$\frac{dA_2(z)}{dz} = i(\beta_2 + C_{22})A_2 + iC_{21}A_1 \quad (2)$$

Where z is the distance along the coupling region of the coupler, A_1 and A_2 are the modal field amplitudes of the LP_{01} mode in the SMF and a certain high-order mode in the FMF, respectively. β_1 and β_2 are the propagation constants of the fundamental mode in the SMF and a certain high-order mode in the FMF, respectively. C_{11} and C_{22} are self-coupling coefficients, C_{12} and C_{21} are mutual-coupling coefficients. C_{11} and C_{22} are negligible with respect to C_{12} and C_{21} and approximately C_{21}=C_{12}=C. The power distributions of the two output ports of the MSC are:

$$P_1(z) = |A_1(z)|^2 = 1 - F^2 \sin^2\left(\frac{C}{F}z\right) \quad (3)$$

$$P_2(z) = F^2 \sin^2\left(\frac{C}{F}z\right) \quad (4)$$

$$F = \left[1 + \frac{(\beta_1 - \beta_2)^2}{4C^2}\right]^{-1/2} \quad (5)$$

Suppose β_2 is the propagation constant of the LP_{11} mode in the TMF, when β_1 is equal to β_2, the phase mismatch $\Delta\beta = \beta_1 - \beta_2$ is equal to 0, indicating that the fundamental mode (LP_{01}) in the SMF and the high-order mode (LP_{11}) in the TMF meet the phase matching conditions. Under phase matching condition, Eqs. 3 and 4 can be simplified as: $P_1(z) = \cos^2(Cz)$ and $P_2(z) = \sin^2(Cz)$ indicating a complete periodic power exchange between the two modes in the lossless case and achieve the conversion between LP_{01} mode and LP_{11} mode.

A. MSC Simulation

Since the propagation constant of the mode varies with the diameter of the fiber, in order to meet the phase matching condition, it is necessary to find the optimum fiber diameter. We calculated the mode effective index versus different fiber diameters by finite element method (FEM) as shown in Fig. 2. There are two kinds of situations that meet the phase matching condition. Firstly, at a diameter of about 22.4 μm, the SMF-LP_{01} curve and the TMF-LP_{11} curve have an intersection point (meeting the phase matching between the LP_{01} mode and the LP_{11} mode). The diameter of SMF and the TMF are pulled to about 22.4 μm directly, which is free of pre-tapering. Secondly, namely the pre-tapered situation. When the diameter of the SMF is less than 6 μm and the diameter of the TMF is less than 9 μm, the effective index curve slope of the LP_{01} mode (in the SMF) equals to that of the LP_{11} mode (in the TMF). The best diameter ratio of the SMF as compared to the TMF is 0.64, so the diameter of the SMF should be pre-tapered to 80 μm.

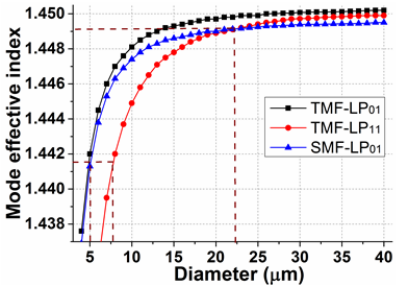

Fig. 2. The mode effective index of the LP_{01} mode (in the SMF) and the LP_{11} mode (in the TMF) versus different fiber diameters at the wavelength of 1064 nm.

We use beam propagation method (BPM) to calculate the modes' propagating in the MSC and confirm two kinds of aforementioned phase matching conditions. As shown in Fig. 3.

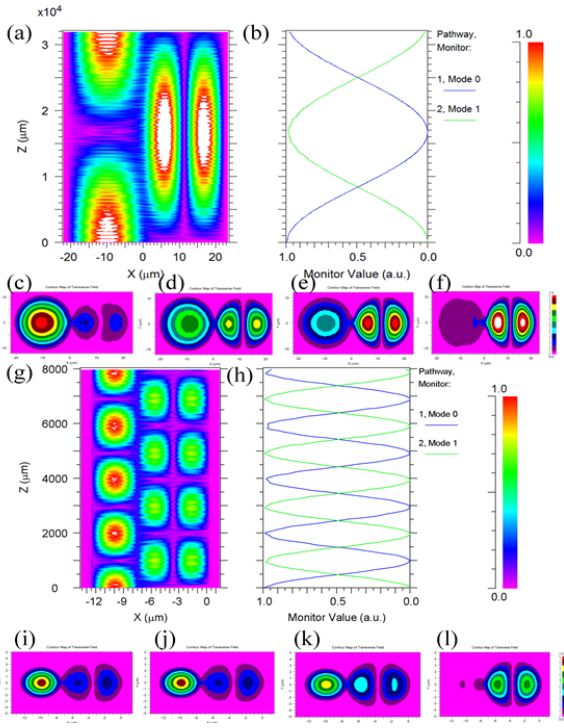

Fig. 3. Simulation results: (a) and (g) mode intensity distribution in the fiber; (b) and (h) Power exchange in the coupling region when LP_{01} mode (in the SMF) converts to LP_{11} mode (in the TMF); (c)-(f) and (i)-(l) Evolutions of the mode field distribution in the coupling region when LP_{01} mode converts to LP_{11} mode in one period.

The simulation results show that the mode power of the LP_{01} mode (in the SMF) and the LP_{11} mode (in the TMF) are periodically exchanged in the coupling region. The diameter of

This article has been accepted for publication in a future issue of this journal, but has not been fully edited. Content may change prior to final publication. Citation information: DOI 10.1109/LPT.2018.2797990, IEEE Photonics Technology Letters

the SMF and the diameter of TMF have the same value of 22.4 μm as shown in Figs. 3(a)-(f). The diameters of SMF and TMF optical fibers are 5 μm and 7.8 μm, respectively (the diameter ratio is about 0.64), as shown Figs. 3(g)-(l).

B. MSC Fabrication

In order to achieve high mode purity, we use weak fusion technique for maintaining the geometry of the SMF and the TMF [21], [25]. Furthermore, unlike other mode selective coupler fabrication techniques for which SMF (or FMF) must be pre-tapered, we use technique free of pre-tapering to fabricate the MSC. The SMF was aligned directly (without pre-tapering) with the TMF and they are fused together using the flame modification method [26]. During the pulling process, a laser source with a wavelength near 1064 nm is launched into the SMF input port. Meanwhile, mode intensity distribution at the TMF output ports is monitored by a CCD camera (CinCam IR, InGaAs). During the pulling process, we can see the intensity distributions of the two-lobed LP_{11} mode on the CCD camera, but the coupling efficiency can only reach about 20%. This is because the phase matching between the LP_{01} mode and LP_{11} mode can only be achieved when both the SMF and the TMF have the same diameter of 22.4 μm. The coupling efficiency depends on the power of the LP_{11} mode From Equation 4, the power of the LP_{11} mode depends on the coupling length z. It can be seen from Fig. 2 that when the two optical fibers have the same diameter of 22.4 μm, the power of the LP_{11} mode reaches the maximum value at a coupling length of about 1.7 cm. However, in our present experiment, the coupling length is only about 0.5 cm when the two fiber diameters are maintained at 22.4 μm, and the coupling efficiency is about 20%. The mode intensity distributions at the TMF output port with different wavelengths are detected by the CCD, as shown in Fig. 4. The purity of the LP_{11} mode is estimated to be above 96% near the wavelength of 1064 nm, measured by the tight bend approach [20]. The LP_{01} mode can be efficiently converted to the LP_{11} mode with a low loss of about 0.5 dB.

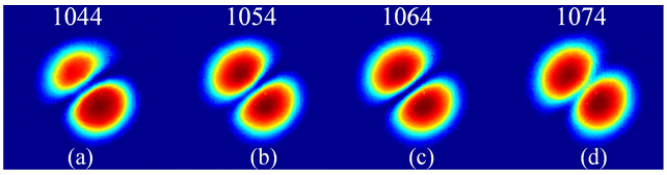

Fig. 4. CCD images of the LP_{11} mode excited in the TMF at different launching wavelengths.

Figs. 5(a) and 5(b) show the microscopic images of the MSC's coupling region and cross-section, measured by a high-precision vertical optical microscope and a horizontal high-precision optical microscope, respectively. It is confirmed that the SMF and the TMF have the same diameter of about 22.4 μm and the coupler cross-section is weakly fused. Thus, the experimental results are in good agreement with the simulation results.

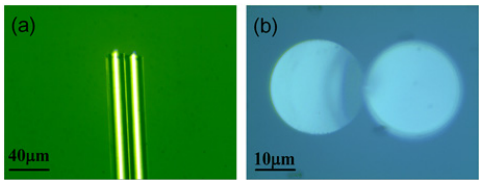

Fig. 5. Microscopic images of the MSC: (a) The coupling region observed by a high-precision vertical optical microscope. (b) The weakly fused coupler cross-section observed by a high-precision horizontal optical microscope.

III. Experimental Setup and Results

A. Experimental Setup

The experimental setup of the CW CVB fiber laser is illustrated in Fig. 6, which consists of one 974 nm laser diode (LD), a 980/1064 nm wavelength division multiplexer (WDM), a section of ytterbium-doped-fiber (YDF, Nufern, SM-YSF-HI), a circulator, a single-mode fiber Bragg grating (SM-FBG), two polarization controllers (PCs) and a MSC. By introducing SM-FBG into the cavity to narrow the bandwidth of the laser, the purity of the CVB is increased [15]. MSC act as transverse mode converter and mode splitter. When the light is reflected by the SM-FBG into the MSC, the LP_{01} mode converted into the LP_{11} mode through a collimator is detected by CCD. The laser spectra are measured by an optical spectrum analyzer (OSA, YOKOGAWA, AQ6370C).

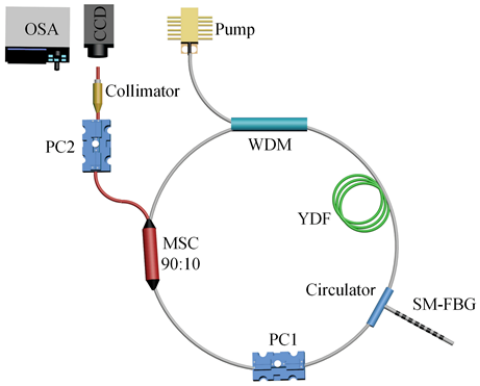

Fig. 6. Experimental setup of the CW CVB fiber laser.

B. Experimental Results

The laser spectrum with a pump power of 120 mW at output is measured as Fig. 7(a). The center wavelength of the laser is 1053.9 nm and the 3-dB bandwidth is measured to be 0.038 nm.

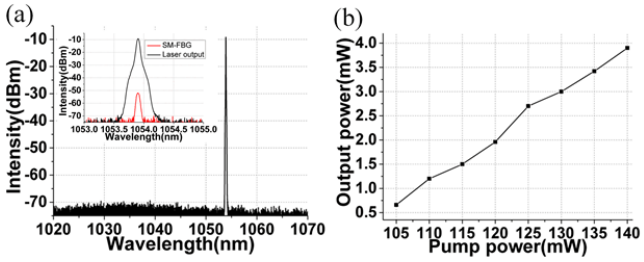

Fig. 7. Experimental results: (a) Optical spectrum of the CW CVB fiber laser (black), inset: compared with the reflective spectrum of a SM-FBG with a 3 dB bandwidth of 0.05 nm (red); (b) Laser output power versus pump power.

The signal-to-background ratio is about 61 dB. Fig. 7(b) shows

This article has been accepted for publication in a future issue of this journal, but has not been fully edited. Content may change prior to final publication. Citation information: DOI 10.1109/LPT.2018.2797990, IEEE Photonics Technology Letters

the laser output power versus the pump power, the slope efficiency of is about 9.1%, which is higher than we have previously proposed passively mode-locked CVB fiber laser based on an MSC [18].

The MSC functions as a mode converter and splitter, when light passes through the MSC, the LP_{01} mode is converted into the LP_{11} mode and output from the TMF fiber output port, which is connected to a collimator and detected by the CCD. The doughnut-shaped intensity profile of the radially and azimuthally polarized beams can be obtained at laser output port through adjustment of PC1 and PC2 as shown in Figs. 8(a) and 8(f). The purity of the radially polarized beam and the azimuthally polarized beam are measured to be 96.6% and 96.3%, respectively [12], [18] .The radially and azimuthally polarized beams could be confirmed by recording the intensity distributions by rotating a liner polarizer inserted between the collimator and the CCD camera. The mode intensity distributions of the radially and azimuthally polarized beams after passing a liner polarizer at different orientations are shown in Figs. 8(b)-8(e) and 8(g)-8(j).

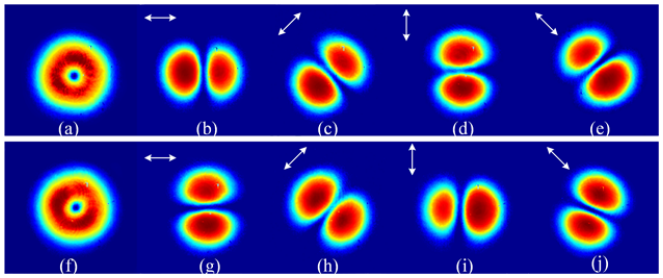

Fig. 8. Intensity distributions of: (a) Radially polarization beam and (f) azimuthally polarization beam without a polarizer; (b)-(e): Radially polarization beam after passing a liner polarizer; (g)-(j): Azimuthally polarization beam after passing a liner polarizer. Arrow indicates the orientation of the linear polarizer.

IV. Conclusion

In summary, we present a CW all-fiber laser generating CVBs with high efficiency and high mode purity near a wavelength of 1.0 μm. A MSC made by a novel weakly fused technology free of pre-tapering is used as the transverse mode converter and mode splitter. The MSC can achieve LP_{11} mode with a high purity of > 96% near wavelength of 1.0 μm with a low loss of about 0.5 dB. The purities of the radially polarized beam and the azimuthally polarized beam are measured to be 96.6% and 96.3%, respectively. The fiber laser works at the wavelength of 1053.9 nm with a 3 dB bandwidth of <0.04 nm and a slope efficiency of > 9%. This simple and novel all-fiber laser source may find applications in many areas such as optical tweezers, optical imaging, and mode-division multiplexed systems.

References

[1] Q. Zhan, "Cylindrical vector beams: from mathematical concepts to applications," *Adv. Opt. Photon.*, vol. 1, no. 1, pp. 1-57, Jan. 2009.

[2] H. Kavauchi, K. Yonezawa, Y. Kozawa, and S. Sato, "Calculation of optical trapping forces on a dielectric sphere in the ray optics regime produced by a radially polarized laser beam," *Opt. Lett.*, vol. 32, no. 13, pp. 1839–1841, Jul. 2007.

[3] R. S. R. Ribeiro, O. Soppera, A. G. Oliva, A. Guerreiro and P. A. Jorge, "New trends on optical fiber tweezers," *J. Lightwave Technol.*, vol. 33, no. 16, pp. 3394-3495, Aug. 2015.

[4] M. Meier, V. Romano, and T. Feurer, "Material processing with pulsed radially and azimuthally polarized laser radiation," *Appl. Phys. A, Solids Surf.,* vol. 86, no. 3, pp. 329–334, Mar. 2006.

[5] L. Novotny, M. R. Beversluis, K. S. Youngworth, and T. G. Brown, "Longitudinal field modes probed by single molecules," *Phys. Rev. Lett.*, vol. 86, no. 23, pp. 5251-5254, Jun. 2001.

[6] A. Bouhelier, F. Ignatovich, and A. Bruyant, "Surface plasmon interference excited by tightly focused laser beams". *Opt. Lett.*, vol. 32, no. 17, pp. 2535-2537, Sep. 2007.

[7] J. L. Li, K. Ueda, and M. Musha, "Generation of radially polarized mode in Yb fiber laser by using a dual conical prism," *Opt. Lett*., vol. 31, no. 20, pp. 2969-2971, Oct. 2006.

[8] M. P. Thirugnanasambandam, Y. Senatsky and K.Ueda, "Generation of radially and azimuthally polarized beams in Yb:YAG laser with intra-cavity lens and birefringent crystal," *Opt. Express,* vol.19 ,no. 3, pp. 1905-1914, Jan. 2011.

[9] S. Ngcobo, I. Litvin, and L. Burger, "A digital laser for on-demand laser modes," *Nature Commun.*, vol. 4, no. 4, pp. 2289, Aug. 2013.

[10] D. Lin, K. Xia, and J. Li, "Efficient, high-power, and radially polarized fiber laser," *Opt. Lett*., vol. 35, no. 13, pp. 2290-2292, Jul. 2010.

[11] H. Wan, H. Li, and C. Wang, "An Injection-Locked Single-Longitudinal-Mode Fiber Ring Laser with Cylindrical Vector Beam Emission," *IEEE Photon. J.* vol. 9, no. 1, pp. 1-8, Feb. 2017.

[12] B. Sun, A. Wang, and L. Xu, "Low-threshold single-wavelength all-fiber laser generating cylindrical vector beams using a few-mode fiber Bragg grating," *Opt. Lett.*, vol. 37, no. 4, pp. 464-466, Feb. 2012.

[13] Y. Zhou, A. Wang, and C. Gu, "Actively mode-locked all fiber laser with cylindrical vector beam output," *Opt. Lett.*, vol. 43, no. 3, pp. 548-550., Feb. 2016.

[14] Y. Zhou, J. Lin, and X. Zhang, "Self-starting passively mode-locked all fiber laser based on carbon nanotubes with radially polarized emission," *Photon. Research*, vol. 4, no. 6, pp. 327-330, Dec. 2016.

[15] B. Sun, A. Wang, and C. Gu, "Mode-locked all-fiber laser producing radially polarized rectangular pulses." *Opt. Lett*. vol. 40, no. 8, pp. 1691-1694, Apr. 2015.

[16] K. Yan, J. Lin, and Y. Zhou, "Bi2Te3 based passively Q-switched fiber laser with cylindrical vector beam emission," *Appl. Opt.*, vol. 55, no. 11, pp. 3026-3029, Apr. 2016.

[17] F. Wang, F. Shi, and T. Wang, "Method of generating femtosecond cylindrical vector beams using broadband mode converter," *IEEE Photon. Technol. Lett.*, vol. 29, no. 9, pp. 1-1, May 2017.

[18] H. Wan, J. Wang, and L. Zhang, "High efficiency mode-locked, cylindrical vector beam fiber laser based on a mode selective coupler," *Opt. Express*, vol. 25, no. 10, pp. 111444-11451, May 2017.

[19] K. Y. Song, I. K. Hwang, and S. H Yun, "High performance fused-type mode selective coupler for two-mode fiber devices," *Opt. Fiber Commun. Conf. IEEE*, vol.1, pp. 32-34, Mar. 2000.

[20] K. Y. Song, I. K. Hwang, and S. H Yun, "High performance fused-type mode-selective coupler using elliptical core two-mode fiber at 1550 nm." *Photon. Technol. Lett. IEEE*, vol. 14, no. 4, pp. 501-503. Apr. 2002.

[21] R. Ismaeel, T. Lee, and B. Oduro, "All-fiber fused directional coupler for highly efficient spatial mode conversion," *Opt. Express*, vol. 22, no. 10, pp. 11610-11611, May 2014.

[22] T. Liu, S. Chen and X. Qi, "High-power transverse-mode-switchable all-fiber picosecond MOPA," Opt. Express, vol. 24, no. 24, pp. 27821-27827, 2016.

[23] S. Kanazawa, Y. Kozawa and S. Sato, "High-power and highly efficient amplification of a radially polarized beam using an Yb-doped double-clad fiber," Opt. Lett., vol. 39, no. 24, pp. 2857-2859, 2014.

[24] Y. L. Xiao, Y. G. Liu, W. Zhi, Z. Wang, and X. Q. Liu, "Design and experimental study of mode selective all-fiber fused mode coupler based on few mode fiber," *Acta. Phys. Sinica.*, vol. 64, no. 20, pp. 204207, Oct. 2015.

[25] G. Pelegrina-Bonilla, K. Hausmann, and H. Sayinc. "Analysis of the modal evolution in fused-type mode-selective fiber couplers," *Opt. Express*, vol. 23, no. 18, pp. 22977-22990, Sep. 2015.

[26] G. Brambilla, "Optical fibre nanowires and microwires: A review," *J. of Opt*., vol. 12, no. 4, pp. 043001, Apr. 2010.